Scintillator Crystal Readout with Wavelength-Shifting Optical Fibers

William Worstell, Steven Doulas, Olof Johnson, and Cheng-Ju Lin
Boston University Physics Department
590 Commonwealth Avenue, Boston, MA 02215

Abstract

Wavelength-shifting fiber readout of scintillator crystals permits efficient discrete event localization over large scintillator areas, by flexibly interfacing position-sensitive photosensors or photosensor arrays to scintillator crystal surfaces. We describe techniques for localizing gamma-ray interactions within large crystals, and for determining the crystal of interaction within multicrystal arrays. Measurements carried out with NaI(Tl) coupled through fibers to photomultipliers confirm the technique's expected light yield, and measurements with BGO coupled through fibers to avalanche photodiodes demonstrate the usefulness of this method for crystal-of-interaction determination. We use a block detector geometry, combining fiber localization with direct energy measurement by large photomultipliers. Potential applications for gamma cameras and for high resolution PET systems are discussed.

I. INTRODUCTION

We have performed initial studies on the readout of inorganic crystal scintillators with wavelength shifting fibers for gamma-ray imaging. This technique can locate gamma-ray interactions within large scintillator crystals, or can identify the crystal-of-interaction within scintillator crystal arrays. Localization within large crystals relates to potential gamma camera applications, while crystal-of-interaction identification may be pertinent to high-resolution PET systems. In either version, we separate the function of localization from that of total energy measurement and timing, using fiber readout for the former purpose and single-PMT readout for the latter purpose. For gamma cameras, waveshifting fiber readout may decrease the number of photomultipliers required, or may decrease the required position-sensitive photosensor area. For PET detectors, it may permit the use of fewer photomultipliers with larger photocathode area, while simultaneously allowing the use of smaller crystals for better spatial resolution. Our preliminary measurements confirm our rough expectations from first principles, but optimal designs will require further work in our choice of scintillator materials, scintillator geometry and coupling, selection of wavelength-shifter fiber characteristics, and choice of photosensor.

II. MATERIALS AND METHODS

A. Fibers and Scintillator Crystals

Scintillator-based gamma-ray imaging systems determine the location of gamma-ray interactions by sensing the distribution of light that emerges from scintillator surfaces. For example, the classic Anger camera [1] finds interaction coordinates from the ratio of light seen by adjacent photomultipliers (PMTs) in a surface PMT array. Within the past decade, several gamma cameras have been developed using single position-sensitive photomultipliers (PS-PMTs) as substitutes for the Anger PMT array [2-5]. These new systems suffer, however, from the PS-PMT's relatively high cost per unit photocathode area, in comparison to conventional photomultipliers. This cost has also prevented high-resolution PET designs incorporating PS-PMTs [6-8] from displacing more conventional block detectors, where the latter use light sharing to determine the crystal-of-interaction [9-11].

Some recent PET designs have used photodiodes to identify the crystal of interaction within a block geometry, at the cost of instrumenting one photodiode channel for each crystal [12]. One group has used large-area avalanche photodiodes both for crystal identification and for energy measurement, at a relatively high cost per channel [13]. We have explored the potential of fluorescent flux concentration, using wavelength shifting fibers, to couple from large-area scintillators to smaller-area photosensors. Optically multiplexing the crystal-of-interaction information from crystal arrays through wavelength shifting fibers reduces the number of instrumented channels, without increasing the level of electronic noise.

Waveshifters are widely used in high-energy physics to concentrate light from large areas onto smaller photosensors. In waveshifters, a fluorescent organic molecule (a dopant within the waveshifter material) absorbs a short-wavelength incident photon, then isotropically emits a secondary longer-wavelength photon. One can use this re-emission process to elude Louisville's theorem by effectively injecting light into a light pipe through the sides of the pipe. In recent years, low-cost plastic wavelength-shifting fibers (WSF) have become available [14], and have been incorporated into a variety of detector designs [15]. These devices combine the waveshifting effect with the compactness and optical transmission efficiency of an optical fiber, as illustrated schematically in Figure 1.

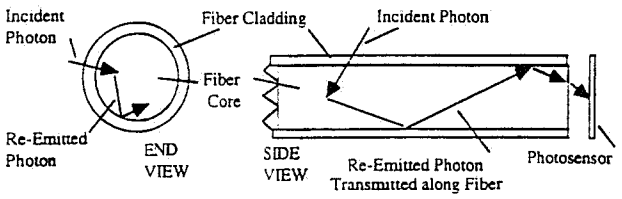

Figure 1: Schematic illustration of light absorption and re-emission within a wavelength-shifting optical fiber.

The refractive index of the fiber core is typically about 1.60, while that of the cladding is about 1.49. For a fiber with this numerical aperture, 4% of the re-emitted light is piped toward each of the two fiber ends, while the remaining 92% of

the re-emitted light exits through the sides of the fiber. The fraction of incident light that is absorbed and re-emitted varies with fiber thickness and dopant concentration, and this concentration is typically set to obtain 90% absorption across a 1mm diameter wavelength shifting fiber.

Wavelength shifting fibers can be used to encode the crystal of interaction within segmented arrays of optically isolated crystals, such as have been used in some high-resolution PET detectors. Perpendicular WSF ribbons coupled to a 2-D crystal array carry information on the interaction crystal's address in two dimensions, as indicated schematically in Figure 2.

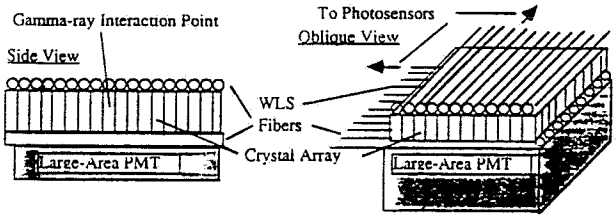

Figure 2: Schematic illustration of crystal-of-interaction identification within a scintillator crystal array, using perpendicular wavelength-shifting fiber ribbons.

By determining which fibers deliver light to a set of position-sensitive or segmented photosensors, one may then determine the crystal of interaction within the array. Because not all the scintillation light is absorbed in passing through a ribbon of WSF, some scintillation light may be sensed by a large-area photomultiplier on the opposite side of a fiber ribbon from the crystal. This large-area photomultiplier may also sense some of the re-emitted light which is not piped in the WSF, and which therefore emerges through the sides of the fibers. This geometry separates the functions of localization (performed with optically multiplexed readout through fibers) and energy measurement (performed with the large-area photomultiplier).

It is also possible to use wavelength-shifting fibers, in conjunction with position-sensitive photosensors, to determine the location of gamma-ray interactions from the profile of light emerging at a large crystal face. Photons striking a polished crystal face at oblique incidence are totally internally reflected, while most photons on trajectories more normal to the crystal face ("direct" light in Figure 3) escape from the crystal.

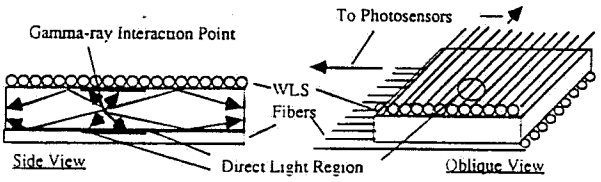

Figure 3: Schematic illustration of interaction localization within a large scintillator crystal, using perpendicular wavelength-shifting fiber ribbons.

Two perpendicular ribbons of wavelength-shifting fibers can then give the position of the gamma-ray interaction in two dimensions, while information on the third coordinate is contained in the width of the fiber hit distribution. An advantage of this technique over direct readout with a position sensitive photosensor is the much smaller position-sensitive photosensor area required for fiber readout

Because a wavelength shifting fiber couples to a crystal all along its length, it optically multiplexes the signal from the crystal into a photosensor. The photosensor area required is thus the fiber thickness times the ribbon width. The disadvantage with respect to direct readout is the small fraction of re-emitted photons which are piped along the fibers. As noted earlier, however, secondary photons that are not captured in the fibers emerge through the sides of the fibers and may be usefully detected with a large-area photosensor. Finally, while a single large crystal and an array of optically isolated small crystals constitute limiting cases for fiber readout, arrays of optically coupled crystals constitute interesting intermediate cases.

Wavelength shifting fibers are available from a number of vendors [16], with a variety of absorption and emission spectra. Technically, scintillating fibers are a subset of wavelength shifting fibers, although the term "waveshifting fiber" or "fluorescent fiber" commonly refers only to fibers which do not scintillate. Within scintillating fibers primary UV light is produced through the recombination of ionized substrate molecules, then absorbed and re-emitted as visible light by a primary fluor. Scintillating fibers incorporating secondary and sometimes tertiary fluors are also available, cascading photons from near UV to blue and then to green, yellow or red wavelengths. Fluor concentrations are adjusted to make this cascade efficient across the fiber diameter.

The final fluorescent absorption and re-emission in a wavelength shifting fiber should have a large Stokes shift in order to avoid self-absorption. Self-absorption results in a shorter attenuation length for the shorter wavelengths of re-emitted light, and for this and other reasons wavelength shifting fibers do not exhibit a single attenuation length. Fiber attenuation curves are typically fitted to the sum of two exponentials, which empirically fit attenuation lengths of order 30cm and 200cm. In the applications discussed below, our fiber lengths are typically short in comparison with either scale, and we may therefore neglect fiber attenuation effects to first order.

B.) Photosensors

A wide range of techniques has been developed for the readout of scintillating and wavelength shifting fibers in high-energy physics applications, employing a variety of photosensors. Some photosensors which have been tested for these applications include discrete photomultiplier (PMT) arrays [17], position-sensitive photomultipliers [18-19], multianode photomultipliers [20-21], avalanche photodiodes (APDs) [22], hybrid APD/PMT devices [23], and APD arrays [24-25]. In typical applications fewer than 50 photons are incident from the fibers onto the photosensor. It should be noted that the light emission efficiency for the plastic scintillator in a typical scintillating fiber is about 4 photons per KeV of energy deposited; this is an order of magnitude below the 40 photons per KeV produced by gamma ray interactions in NaI(Tl). About 200 KeV is deposited in a 1mm fiber by the passage of a single minimum ionizing particle, which combines with the 4% trapping fraction per

end and the above scintillator efficiency to yield about 32 photons per minimum ionizing particle. When collected by a PMT with a bialkali photocathode, this generates fewer than 8 photoelectrons (even before allowing for fiber attenuation effects). Despite these low light levels, fiber tracking technology is being extensively developed for high-energy physics applications [26], thereby contributing to demand for low-cost fiber readout photosensors with low noise.

In our technique of coupling crystal scintillators to wavelength shifting fibers for gamma-ray imaging, we begin with the advantage of a higher intrinsic scintillation efficiency in the crystal scintillator relative to scintillating fibers. This advantage is partially mitigated by some inefficiency in coupling scintillation light from the crystal to the fibers. The net result is light levels well within the reach of new and developing scintillating-fiber sensor technologies.

Low-noise avalanche photodiodes and APD arrays represent an emerging technology which is particularly interesting for fiber readout generally, and for this technique in particular. Bialkali photocathodes such as those usually used with photomultipliers have a peak quantum efficiency of about 25% for blue (410nm) light, typically falling to about 15% for green (500nm) light and below 5% for yellow (570nm) light.[27] Although one may obtain conventional photomultipliers with enhanced spectral sensitivities at longer wavelengths (green extended and multialkali red extended PMTs), position-sensitive and multianode PMTs are currently only available with normal bialkali photocathodes. By contrast, semiconductor photosensors such as avalanche photodiodes can have a quantum efficiency as high as 50% for blue light, increasing to 60% for green light and reaching 70-80% for red light.[24] Avalanche photodiodes, when operaed with an internal gain of several hundred, can significantly improve signal-to-noise at low light levels relative to PIN photodiodes and other unity gain photosensors. The increase in leakage current and capacitance noise with device active area initially kept the size of commercially available APDs to $< 1mm^2$, but advances in fabrication technology have resulted in relatively low-noise devices of up to 2.5cm diameter. These large-area APDs have recently been incorporated into segmented arrays with up to 64 pixels (each 3mm x 3mm) on a single device [23-24], giving rise to the prospect of dramatically reduced costs per APD channel.

Leakage currents result in shot noise from an APD, with the rms fluctuation in this leakage current of order 140 electrons/100 nanoseconds for a typical device operating at room temperature. This noise increases like the square root of the shaping time, and is very sensitive to the APD temperature. A typical device will show a 10-fold reduction in rms leakage (noise equivalent power) for a 40° C decrease in temperature. APDs may be readily cooled to -50° C, which reduces the noise equivalent power by two orders of magnitude below its room temperature value [28]. With WSF fiber readout, it is possible to cool APDs while leaving the scintillator crystals at room temperature, because of the low thermal conductivity and small cross-sectional area of the fibers.

The sensitivity of an avalanche photodiode to low light levels is ultimately determined by noise within the APD, given a sufficiently low-noise charge-sensitive preamplifier. Given a typical APD capacitance of 130 pF/cm^2, a charge-sensitive preamplifier with feedback capacitance of 1pF and capacitance from input to ground of 50 pF may be combined with a 0.5 cm^2 APD to yield output noise as low as 100 electrons rms in a 200ns window. [13, 30-32] For an APD operating with a gain of several hundred, this would correspond to a detector input noise of less than one electron. In most implementations, therefore, amplifier noise will be dominated by leakage currents and by thermal excitation of e/h pairs initiating avalanches within the APD. For a 200 nanosecond shaping time (appropriate for BGO) and APD operation at -50° C, we expect only about 3 photoelectrons of rms shot noise and less than 1 photoelectron of amplifier noise for the above parameters. At this noise level, a cooled APD can trigger on fewer than 20 photons with good efficiency and low accidental rates. This predicted sensitivity agrees with that observed by manufacturers of these devices [32], and is consistent with our measurements on BGO coupled to APDs through red WSF ribbons, as discussed below.

III. PRELIMINARY RESULTS

We have performed measurements which confirm the light yield expected for WSF readout of NaI(Tl) crystals with PMTs, and have measured crystal-of-interaction trigger efficiency and noise for WSF readout of BGO crystals using APDs. In each instance we have not fully optimized system parameters such as WSF characteristics (choice of fluor and fluor concentration, fiber lengths, and treatment of fiber ends) coupling from crystal to WSF, or coupling from WSF to photosensor. Our results therefore generally give a lower bound on achievable system performance for the configurations which were tested. For the tests involving APDs, further optimization in choice of APD characteristics and operating conditions, plus choice of preamplifier characteristics, are expected to yield some performance improvements. While our initial results clearly demonstrate the feasibility of WSF readout for some choices of scintillator and photosensors, and while we can use these results to extrapolate to intrinsic limitations on system performance, full determination of this technique's practical performance limitations must await further optimization.

A.) NaI(Tl) and PMT Readout

A key performance parameter for designs based on the WSF readout method is the light yield at the fiber ends. We have made measurements with NaI(Tl) crystals read out through a ribbon of 1mm diameter round WSF coupled to a PMT with a bialkali photocathode; a rough schematic of our apparatus is given in Figure 4 below.

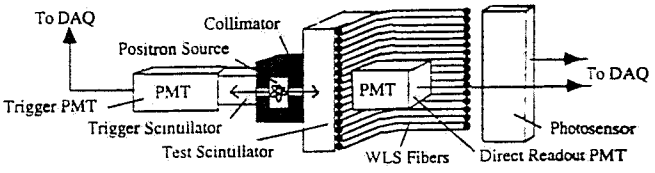

Figure 4: Apparatus used to measure light yield and photosensor response for gamma ray interactions in scintillators coupled to waveshifting fibers.

A Na^{22} positron source generates pairs of back-to-back annihilation gamma rays, where one member of each pair is collimated and detected with a trigger scintillator (a thick piece of fast plastic scintillator) coupled to a trigger PMT. The companion gamma ray enters the scintillator under test, where it interacts to produce scintillation light. Most wavelength-shifted light emerges through the sides of the WSF ribbon, and may be sensed with a direct readout PMT; this PMT also measures the direct light production of the crystal when the WSF ribbon is removed from the apparatus. That light which is piped along the WSF is read out with a second photosensor (either a single large PMT or an APD). For the NaI(Tl) measurements, pulse amplitudes were digitized by a charge-sensitive ADC (LeCroy Research Systems model 2249W) with a 1 microsecond gate width, and were recorded by a CAMAC-based computer data acquisition system (DAQ). Photomultiplier gains were calibrated with a light-emitting diode (LED), using the approximation that observed pulse height fluctuations at low light levels were entirely due to photoelectron statistics. We estimate the error in this absolute calibration as 10% or less.

Our non-optimized NaI(Tl)/WSF system collected more than 60 photoelectrons (PEs) at the fiber readout per 511 MeV gamma ray interaction, as shown in Figure 5. This was obtained while reading out a single end of the green WSF ribbon (the opposite fiber end was cut and polished, but not mirrored) using a PMT having about 15% quantum efficiency for green light. The NaI(Tl) crystal had 5 surfaces coated with diffuse reflective paint, and was sealed behind a 3mm thick glass plate. This glass plate was then coupled to the WSF ribbon with optical grease, and one polished end of the WSF ribbon was coupled to a PMT with optical grease. Direct readout of the same crystal's blue light (coupling the glass plate to a PMT with grease) gave 2600 PEs.

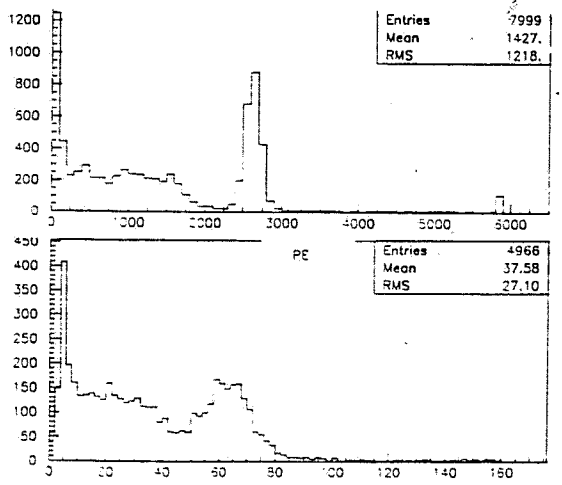

Figure 5: Measured light yield for NaI(Tl) and 511 keV gammas: a) coupled directly to photomultiplier, and b) coupled through wavelength shifting fibers to photomultiplier.

Given the 40 photons/keV from NaI(Tl) and the PMT's 25% quantum efficiency for blue NaI(Tl) light, direct readout therefore collected about 50% of the available light. We measured that 80% of the blue scintillation light incident on the WSF ribbon was absorbed in a single pass through the ribbon; this measurement required using a variety of cutoff filters to observe the wavelength distribution of that light which was not absorbed, in order to correct for the direct PMT's collection of re-emitted green light. The round WSF we used has a 4% per end capture fraction, and fiber attenuation was not significant for the short ribbons used in this test. Combining the above factors, we predict 330 photons (= 40 x 511 x .50 x .80 x .04) per fiber ribbon end with NaI(Tl) and green WSF, corresponding to about 50 photoelectrons at 15% quantum efficiency. Our measurements with this system therefore confirmed this prediction at the 20% level. We attribute the slight excess of observed over expected light collection to short fiber lengths from crystal to photosensors, causing the collection of some "un-piped" light.. Reading out through a 30cm long fiber ribbon reduced this yield to 40 photoelectrons.

B.) BGO and APD Readout

A similar calculation of the light yield for a given scintillator/WSF/photosensor combination may be carried out in predicting the expected capability of this technique for crystal-of-interaction determination in optically segmented systems. For example, BGO produces about 7 photons/keV, so that a 511 keV gamma ray photocapture results in the production of about 3600 scintillation photons within the crystal. Using a BGO crystal wrapped on four surfaces with diffuse reflectors, we measured about 200 photoelectrons with the BGO coupled directly to a photomultiplier with optical grease. Given the roughly 15% average quantum efficiency of the PMT across the BGO emission spectrum, this corresponds to more than 1300 photons emerging from each unwrapped crystal surface. This implies 37% light collection per end, roughly consistent with measurements performed on similarly-wrapped crystals by other groups [12, 33]. To wavelength-shift the green scintillation light, we have used red WSF (Bicron type R-17).

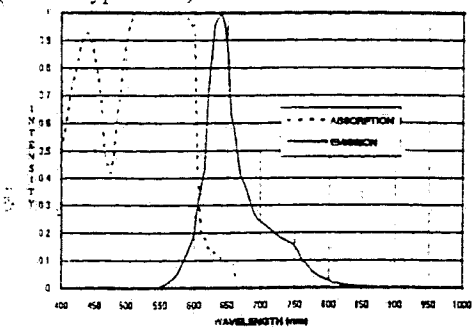

Figure 6: Absorption and emission spectra for Bicron RED-17 wavelength shifting fibers used to couple BGO to APDs.

The absorption and emission spectra for these fibers is shown in Figure 6, with an absorption maximum near 540nm and an emission maximum near 630nm. We measured the efficiency for a ribbon of this particular WSF to absorb and re-emit BGO light traversing a 3/4mm thick ribbon as roughly 50%. To boost the light collection, we mirrored one end of each fiber in the WSF ribbon, resulting in collection of roughly 7% of the re-emitted light. We therefore estimate the light emerging from the fibers as about 40 photons.

The light from the fibers was coupled across an air gap to a cooled large-area avalanche photodiode, read out through a

Canberra 2004 pre-amplifier and a EG&G ORTEC 474 Timing Filter amplifier with a 200ns time constant. The output from this shaping amplifier was then collected with a charge-sensitive ADC (LRS 2249W) with a 2-microsecond gate width. The APD was operated at a gain of about 100, and was cooled with dry ice. APDs from two vendors were tested (Advanced Photonics Model #394-70-72-501 and Radiation Monitoring Devices Model #SH2S-HG), and the two devices performed comparably. Figure 7 shows the APD pulse height distribution in response to 511 keV gamma interactions and to background triggers

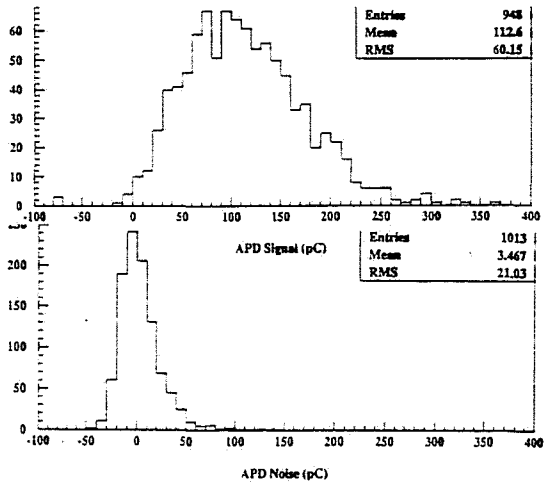

Figure 7: Cooled APD pulse amplitude for: a) 511 keV gamma photocapture in BGO crystal (signal), and b) no interaction in crystal (background).

A cut on each distribution at 50 picocoulombs results in 90% efficiency for signal and less than 5% false triggers from noise. The width of the noise peak primarily reflects electronic noise in the preamplifier and shaping amplifier, which dominates over APD noise once the APD is sufficiently cooled. The width of the signal peak results from a combination of photostatistics, APD multiplication noise, and a small contribution from electronic noise; the relative contributions to this signal's width are under continuing study. Better coupling from the WSF to the APD and higher efficiency for absorbing BGO light in the WSF ribbon may both be expected to increase the light yield and thereby improve performance. Nonetheless, clean identification of the crystal of interaction has already been achieved with this simple system, before optimization.

IV. DISCUSSION

We have performed measurements with the most commonly used scintillators for gamma cameras and for PET, NaI(Tl) and BGO, coupled to appropriate WSF ribbons and photosensors. This technique is capable of more general application, however. New, fast scintillators such as YALO [33] and LSO [34] are also of interest, as well as other bright scintillators like CsI(Tl). The decay times of the fluors within WSF are typically less than 10ns, as are the response times for either PMT or APD photosensors, preserving the speed of the new fast crystals. Many of the fast Cerium-doped crystals are UV emitters, permitting wavelength shifting either to blue light (for PMT readout) or to longer wavelengths (for APD readout). Large-area readout of wavelength shifted light from the sides of the WSF ribbons allows relatively efficient UV-emitting crystal readout without requiring expensive quartz window photomultipliers. For potential gamma camera applications, use of non-hygroscopic crystals would facilitate efficient fiber coupling to the surfaces of large, flat crystals.

The spatial resolution achievable with this method can be no better than the width of the light distribution emerging from the crystal, divided by the square root of the number of photoelectrons. Unfortunately, NaI(Tl) crystals mounted either for Anger cameras or for PS-PMT readout have their light distribution broadened by a diffuse reflector on the entry window to the crystal. Since the system resolution for these devices is limited by their collimator aperture and the distance to the patient, very fine spatial resolution for their crystal/photosensor system is not needed. However, cameras using PS-PMTs (which employ a hardware centroid readout) have observed significantly degraded resolution for large crystals due to outlying hits from diffusely reflected photons [4]. Since WSF readout collects only 8% as many photoelectrons as does direct coupling, obtaining spatial resolution comparable to the 4mm FWHM achieved with PS-PMT devices would require narrowing of the light distribution exiting the crystal, possibly combined with pixellated photosensor readout. Crystals without reflectors and with all surfaces polished may have useful optical properties for position-sensitive readout of large crystals. The energy resolution obtainable for such a configuration is of course also a concern. We have been unable to obtain NaI(Tl) crystals in this geometry, but measurements which we have begun on YALO and CsI(Tl) crystals should provide quantitative details soon.

Crystal-of-interaction determination among optically isolated crystals is simpler than event localization within large crystals, since it only requires triggering on light collection above threshold from a set of signal fibers. Fiber readout through photosensors with bialkali photocathodes is in practice restricted to blue or green WSF, because of the poor quantum efficiencies of these devices for yellow or red light. To read out a crystal such as BGO, which emits green light (which must then be shifted to yellow or red within the fibers), semiconductor photosensors such as avalanche photodiodes are much more efficient than photomultipliers.

Since low-noise avalanche photodiodes currently cost several hundred dollars each, multiplexing of fibers onto readout channels is important for a cost-effective implementation. To this end, it is important to note that coupling the two opposite ends of fibers to separate photosensors may allow 2N photosensors to read out N^2 fibers. If two perpendicular ribbons are read out in this way, 4N APDs could in principle read out N^4 optically isolated crystals. Achieving this is practice may require more efficient absorption of BGO light by WSF ribbons, and will also require more careful optimization of optical couplings and APD operating conditions. We have recently begun work on such an imaging BGO crystal array. The results we have reported from our single-channel prototype give us confidence that this level of photosensor multiplexing should be possible without an excessive number of background hits, for sensing 511 keV gamma ray interactions in BGO crystals.

V. CONCLUSIONS

Readout of inorganic crystal scintillators through wavelength shifting fibers shows some promise for gamma-ray imaging, both in interaction localization within large crystals and in crystal-of-interaction determination within scintillator crystal arrays. In either implementation, a large parameter space remains to be optimized including scintillator type, coupling optics, wavelength-shifting fiber characteristics, and choice of photosensor. Measurements with NaI(Tl) coupled to green fibers and a photomultiplier confirm that the light yield of such systems can be simply predicted with good accuracy. Measurements with BGO coupled to red fibers and APDs have demonstrated the potential of this technique for determining crystal-of-interaction in response to 511 keV gamma rays. The achievable level of spatial resolution and of photosensor multiplexing (which drives the system cost) requires further system optimization before it can be accurately determined. We are continuing work on such optimization with a variety of scintillators, wavelength shifting fibers, and photosensors.

ACKNOWLEDGMENTS

We would like to thank Jan Vasiliev of the Budker Institute for Nuclear Physics in Novosibirsk, Russia, for providing us with BGO samples, and to thank Bicron Corporation for providing us with samples of their RED-17 wavelength shifting fiber. We would also like to thank Richard Farrell of Radiation Monitoring Devices for useful discussions about APDs, and to thank Charles Burnham of Massachusetts General Hospital for helpful discussions regarding PET systems. This work was supported in part by the U.S. Department of Energy under Grant No. DE-FG02-91ER40676, and in part by the Boston University Center for Photonics Research, enabled under Grant No. N00014-93-1-1186 from the Office of Naval Research.

REFERENCES

1 H.O. Anger, "Scintillation Camera", Rev. Sci. Instru. 29, 17 (1958)

2 J. Rogers, "Testing an Improved Scintillation Camera for PET and SPECT", IEEE Trans. Nucl. Sci., 33, 519 (1986)

3 N. Yasillo, R. Beck and M. Cooper, "Design Considerations for a Single Tube Gamma Camera", IEEE Trans. Nucl. Sci. 37, 609 (1990).

4 Z. He, A. Bird, D. Ramsden, and Y. Meng, "A 5 Inch Diameter Position-Sensitive Scintillation Counter", IEEE Trans. Nucl. Sci., 40, 447 (1993).

5 N. Yasillo, R. Mintzer, J. Aarsvold, K. Matthews, S. Heimsath, C. Ordonez, X. Pan, C. Wu, T. Block, R. Beck, C-T Chen, and M. Cooper, "A Single-Tube Miniature Gamma Camera", IEEE Trans. Nucl. Sci., 41, 1073 (1994).

6 M. Singh, R. Leahy, K. Oshio, R. Brechner and X. Yan, "A New Generation of SPECT and PET Systems Based on Position Sensitive Photomultipliers", IEEE Trans. Nucl. Sci. 37, 1321 (1990).

7 T. Yamashita, M. Watanabe, K. Shimizu and H. Uchida, "High Resolution Block Detectors for PET", IEEE Trans. Nucl. Sci., 37, 589 (1990).

8 M. Watanabe, H. Uchida, H. Okada, K. Shimizu, N. Satoh, E. Yoshikawa, T. Ohmura, T. Yamashita, and E. Tanaka, "A High Resolution PET for Animal Studies", IEEE Trans. Med. Imag., 11, 577, (1992).

9 J. Rogers, A. Taylor, M. Rahimi, R. Nutt, M. Andreaco, C. Williams, "An Improved Multicrystal 2-D BGO Detector for PET", IEEE Trans. Nucl. Sci., 39, 1063, (1992).

10 W-H. Wong, "A Positron Camera Detector Design with Cross-Coupled Scintillators and Quadrant Sharing Photomultipliers", IEEE Trans. Nucl. Sci. 40, 962 (1993).

11 M. Tornai, G. Germano, G. Hoffman, "Positioning and Energy Response of PET Block Detectors with Different Light Sharing Schemes", IEEE Trans. Nucl. Sci. 41, 1126, (1994).

12 W. Moses, S. Derenzo, R. Nutt, W. Digby, C. Williams, and M. Andreaco, "Performance of a PET Detector Module Utilizing an Array of Silicon Photodiodes to Identify the Crystal of Interaction", IEEE Trans. Nuucl. Sci. 40, 1036 (1993).

13 A. Lightstone, R. McIntyre, R. Lecomte, D. Wchmitt, "A Bismuth Germanate-Avalanche Photodiode Module Designed for Use in High Resolution Positron Emission Tomography", IEEE Trans. Nucl. Sci., 33, 456 (1986); C. Carrier and R. Lecomte, "Recent Results in Scintillation Detection with Silicon Avalanche Photodiodes", IEEE Trans. Nucl. Sci., 37, 209 (1990); R. Lecomte, J. Cadorette, P. Richard, S. Rodrigue, D. Rouleau, "Design and Engineering Aspects of Avalanche Photodiode PET Tomograph", IEEE Trans. Nucl. Sci., 41, 1063 (1994).

14 T. White, "Scintillating Fibers", Nucl. Inst. Meth. A273, 820 (1988).

15 R. Wojcik, B. Kross, S. Majewski, A. Weisenberger, C. Zorn, "Embedded Waveshifting Fiber Readout of Long Scintillators", Nucl. Inst. Meth. A342, 416 (1994) and references therein.

16 Bicron Corporation, 12345 Kinsgman Rd., Newbury, OH 44065; Kuraray International Corporation, 200 Park Avenue, New York, NY 10166; Optectron, Inc., 91946 Les Ulis, France.

17 A. Weisenberger, F. Cheung, B. Kross, S. Majewski, R. Wojcik, C. Zorn, "Optimization of the Use of Small Inexpensive Side-Window Photomultiplier Tubes for Scintillator Readout", IEEE Trans. Nucl. Sci. 41, 681 (1994); A. Weisenberger, A. Day, J. Houck, B. Kross, S. Majewski, M. Piller, R. Wojcik, C. Zorn, "Low Cross-Talk Fiber Readout of Scintillating Detectors, IEEE Trans. Nucl. Sci. 40, 455 (1993); A. Weisenberger et. al. "Application of Small Inexpensive Side-on (Side-window) Photomultiplier Tubes for Scintillating Fiber Readout, IEEE Trans. Nucl. Sci., 39, 666 (1992).

18 J. Bahr, B. Hoffman, H. Ludecke, R. Nahnhauer, M. Pohl, H.-E. Roloff, "Test of a position-sensitive photomultiplier for fast scintillating fiber detector read-out", Nucl. Inst. and Meth., A330, 103 (1993).

19 A. Gorin, "Fast readout of scintillating fibres using position-sensitive photomultipliers", Nucl. Inst. Meth. A344, 220 (1994).

20 A. Murakami, H. Yoshinaka, S. Sahu, A. Maki, H. Yamaguchi, N. Zhang, "Signal Readout from Scintillating Fiber by Using Multianode Photomultiplier Tubes", IEEE Trans. Nucl. Sci., 40, 490 (1993).

21 M. Salomon, "New Measurements of Scintillating Fibers Coupled to Multianode Photomultipliers", IEEE Trans. Nucl. Sci., 39, 671 (1992).

22 M. Salomon and J. Kitching, "Preliminary Results on the Use of Avalanche Photodiodes for Scintillating Fiber Readout", IEEE Trans. Nucl. Sci., 38, 140 (1991).

23 P. Cushman, R. Rusack, "A 64 Channel Photomultiplier Tube with an Electron Bombarded Avalanche Photodiode", contribution to the IEEE Nucl. Sci. Symposium, 1993.

24 M. Squillante, R. Farrell, J. Lund, F. Sinclair, G. Entine, K. Keller, "Avalanche Diode Low Energy X-ray and Nuclear Partiocle Detector", IEEE Trans. Nucl. Sci. 33, 336 (1986); M. Squillante, J. Gordon, R. Farrell, S. Vasile, K. Daley, C. Oakes, K. Vanderpuye, "Recent Advances in Avalanche Photodiode Technology", SPIE Vol 2009 X-ray Detector Physics and Applications II (1993).

25 E. Gramsch, M. Szawlowski, S. Zhang, M. Madden, "Fast, High Density Avalanche Photodiode Array", IEEE Trans. Nucl. Sci., 41, 457 (1994).

26 Workshop on Scintillating Fiber Detector Development for the SSC, (Fermilab, Nov. 1988); R. Nahnhauer (ed.) Workshop on Application of Scintillating Fibers in Particle Physics, Blossin, (1990); R. Ruchti (ed.) Workshop on Application of Scintillating Fibers in Particle Physics, Notre Dame (1994).

27 PMT product information from: Hamamatsu Corp., 360 Foothill Rd., Bridgewater, NJ 08807; Thorn Emi Electron Tubes Inc., 100 Forge Way, Rockaway, NJ 07866, Phillips Scientific, 150 Hilltop Rd., Ramsey, NJ 07446; Burle Industries, 1000 New Holland Ave., Lancaster, PA 17601-5688.

28 APD product information from: Radiation Monitoring Devices, Inc., 44 Hunt St., Watertown, MA 02172; Advanced Photonix, Inc., 1240 Avenida Acaso, Camarillo, CA 93012.

29 R. Burnham and D. Scarl, "Detection of deep-red low-level light pulses", Applied Optics, 25, 1514 (1986).

30 G. Entine, G. Reiff, M. Squillante, H. Serreze, S. Lis, G. Huth, "Scintillation Detectors using Large Area Silicon Avalanche Photodiodes", IEEE Trans. Nucl. Sci., 30, 431 (1983).

31 K. James, M. Masterson R. Farrell, "Performance evaluation of new large-area avalanche photodiodes for Scintillation Spectroscopy", Nucl. Inst. Meth. A313, 196 (1992).

32 R. Farrell, private communication.

33 S. Ziegler, J. Rogers, V. Selivanov, I. Sinitzin, "Characteristics of the New YAlO3:Ce Compared with BGO and GSO", IEEE Trans. Nucl. Sci., 40, 194 (1993).

34 C. Melcher, J. Schweitzer, "A promising new scintillator: cerium doped lutetium oxyorthosilicate", Nucl. Instr. Meth., A314, 212 (1992); P. Dorenbos, J. de Haas, C. van Eijk, C. Melcher, J. Schweitzer, "Non-linear response in the scintillation yield of Lu2SiO5:Ce3+", IEEE. Trans. Nucl. Sci. 41, 714 (1994).